Supporting information

Highly Active Co-N-doped Graphene as an Efficient Bifunctional Electrocatalysts (ORR/HER) for Flexible All-Solid-State Zinc-Air Batteries

Hai-Lang Jia,[‡,*] Jiao Zhao,[‡] Lei Gu, Zhi-Jie Peng, Zheng-Lv Bao, Xuan-Long Sun, Ming-Yun Guan[*]

School of Chemical and Environmental Engineering, Institute of Advanced Functional Materials for Energy, Jiangsu University of Technology, Changzhou 213001, P. R. China.

Electrochemical measurements

A conventional three-electrode system was employed to evaluate the electro-catalytic performance of the obtained catalyst on a CHI 760E electrochemical workstation. A rotating disk electrode (RDE) with a glassy carbon (GC) disk (electrode area: 0.1256 cm^2) was used as the working electrode, Ag/AgCl was used as the reference electrode, and platinum wire (ORR) or graphite (HER) was used as the counter electrode. The rotating ring disk electrode measurements for ORR were carried out on RRDE in a N_2 or O_2-saturated 0.1 M KOH electrolyte solution at a scan rate of 10 mV/s at various rotation rates of 400, 600, 900, 1200, 1600 rpm. Linear sweep voltammetry (LSV) at a scan rate of 10 mV/s was conducted in 0.1 M KOH at room temperature. Before the electrochemical measurements, the electrolyte solution was purged with O_2 for 30 min to achieve an O_2-saturated solution, and stable polarization curves were recorded after 20 cycles. All the potentials were converted to the potential versus the reversible hydrogen electrode (RHE) according to E_{vs}RHE = E_{vs}Ag/AgCl + $E_{ø}$Ag/AgCl + 0.059 pH. The RDE measurements were performed at different rotating speeds from 400 to 1600 rpm at a scan rate of 10 mV s^{-1}. Koutecky-Levich plots were used to investigate the effective electron-transfer number and the mass-transport corrected current density for ORR at different potentials. According to the Koutecky-Levich equation:

$$\frac{1}{J}=\frac{1}{J_K}+\frac{1}{J_L}=\frac{1}{J_k}+\frac{1}{Bw^{1/2}} \quad (1)$$

$$B = 0.62nFC_0(D_0)^{2/3}v^{-1/6} \quad (2)$$

$$J_k=nFkC_0 \quad (3)$$

Where ω is the angular velocity, J is the measured current density, J_K and J_L are the kinetic and diffusion-limiting current densities. F is Faraday constant (96485 C mol^{-1}), D_0 is the diffusion coefficient of O_2 (1.9×10^{-5} cm^2 s^{-1}), v is the kinetic viscosity of the electrolyte (0.01 cm^2 s^{-1}) and C_0 is the bulk concentration of O_2 (1.2×10^{-6} mol

cm^{-3}), n is the electron transfer number. B can be determined from the slope of the K-L plots, and then the electron transfer number n can be obtained.

Rotating ring-disk electrode (RRDE) measurements were recorded with catalyst inks and electrodes prepared by the same method as that for the RDE measurements. The H_2O_2 produced and the electron number (n) transferred during the ORR were calculated using the following equations:

$$n = 4\frac{I_D}{I_D + I_R/N}$$

$$H_2O_2\% = 100 \times \frac{4 - n}{2}$$

The rotating ring-disk electrode was employed to detect the H_2O_2 yield, where the ring potential was set to 1.3 V (vs. RHE). where I_D is the Faradaic current at the disk, I_R is the Faradaic current at the ring, and N= 0.37 is the collection efficiency of ring electrode.

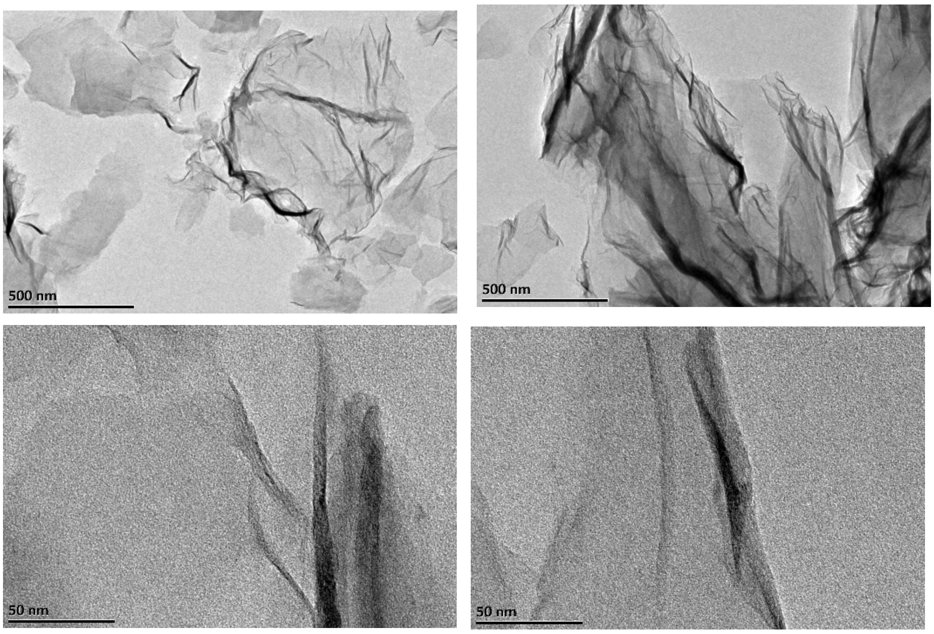

Fig. S1 HR-TEM of Co-N-C/rGO.

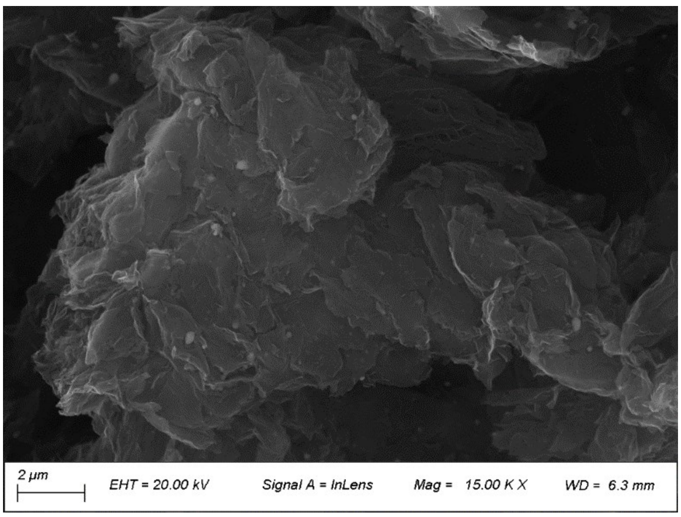

Fig. S2 SEM of Co-C/rGO.

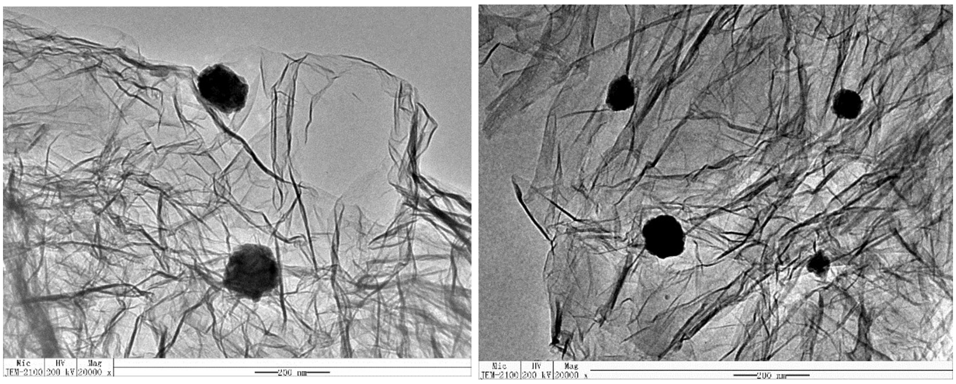

Fig. S3 TEM of Co-C/rGO.

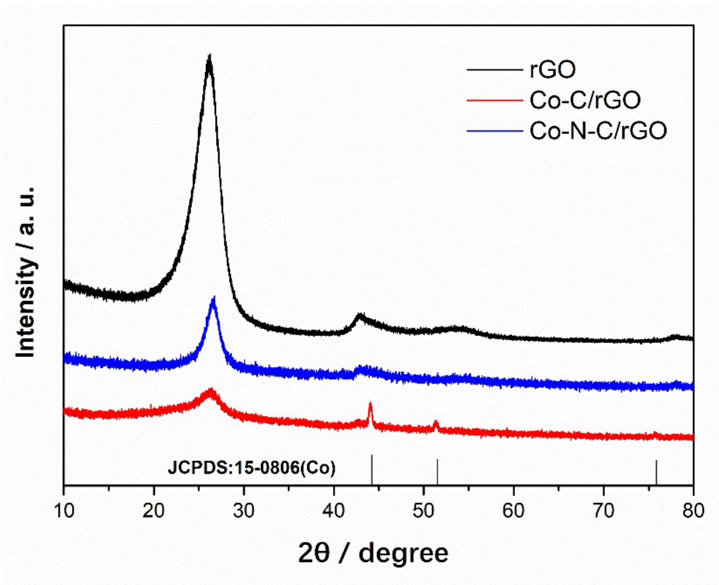

Fig. S4 XRD patterns of Co-N-C/rGO, Co-C/rGO, rGO

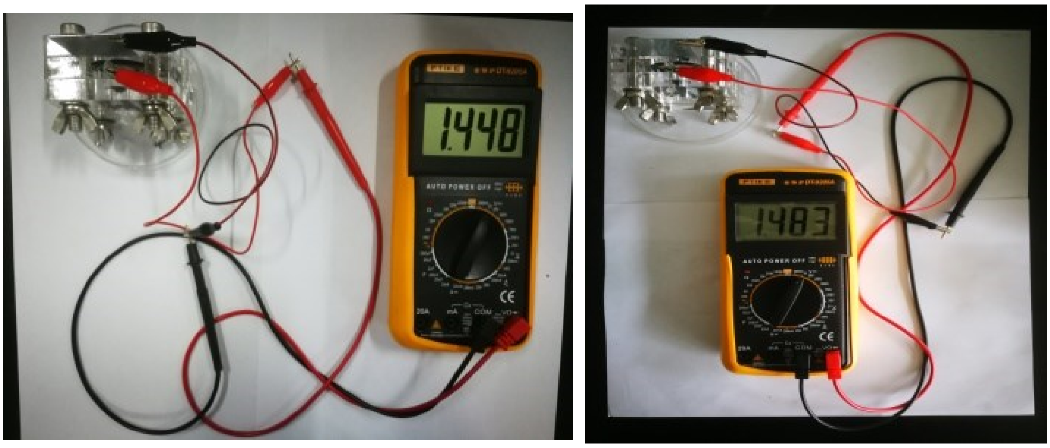

Fig. S5 Opencircuit voltages of commercial Pt/C (left) and Co-N-C/rGO (right) based primary liquid ZABs

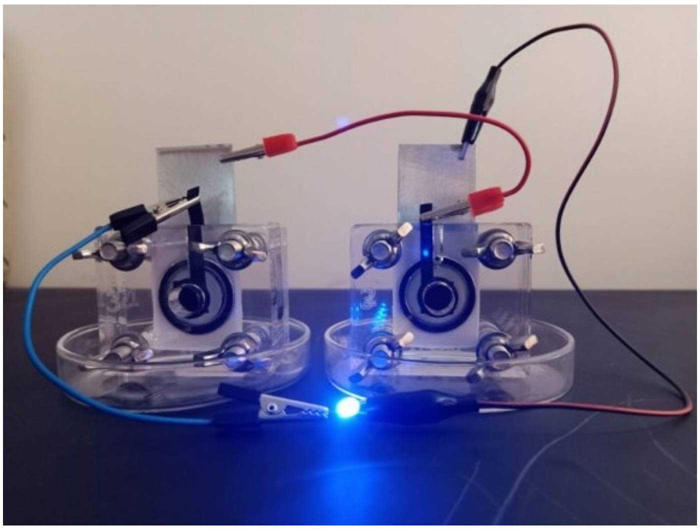

Fig. S6 Two Zn-air batteries were connected in series to supply adequate voltage to power the colored LEDs (2.5 V).

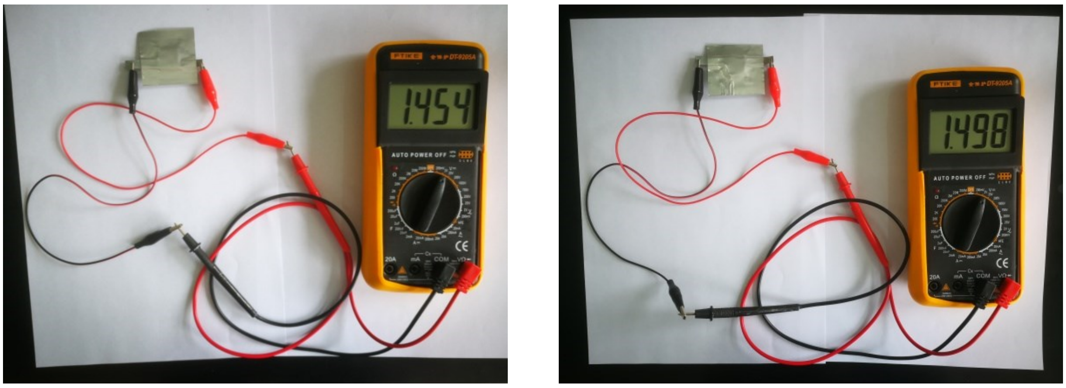

Fig. S7 Opencircuit voltages of commercial Pt/C (left) and Co-N-C/rGO (right) based flexible all-solid-state ZABs

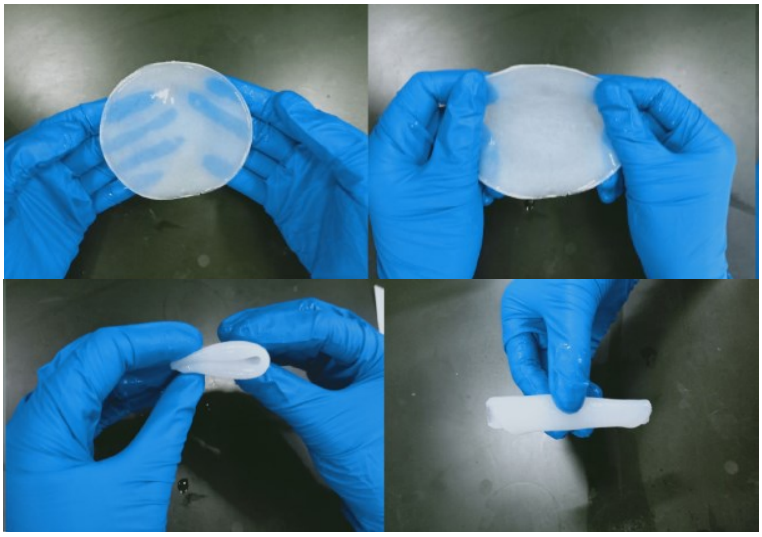

Fig. S8 Images of PVA+PEO solid electrolyte under various mechanical deformations

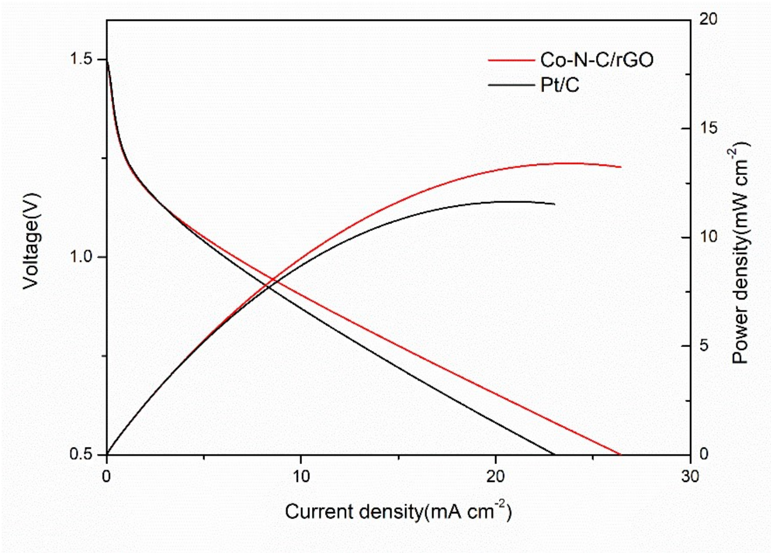

Fig. S9 Polarization and power density curves of Pt/C and Co-N-C/rGO based flexible all-solid-state ZABs with PVA+PEO solid electrolyte

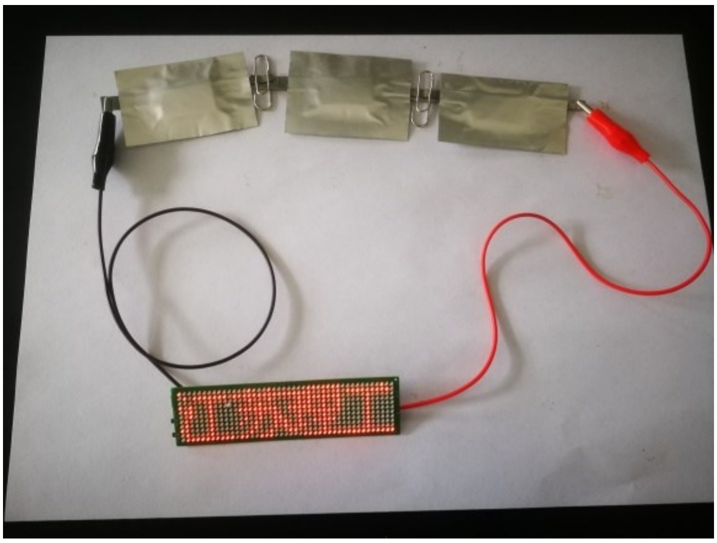

Fig. S10 Images of the Co-N-C/rGO based flexible all-solid-state ZABs in series power a light emitting diode (LED) array (3.7-5 V)

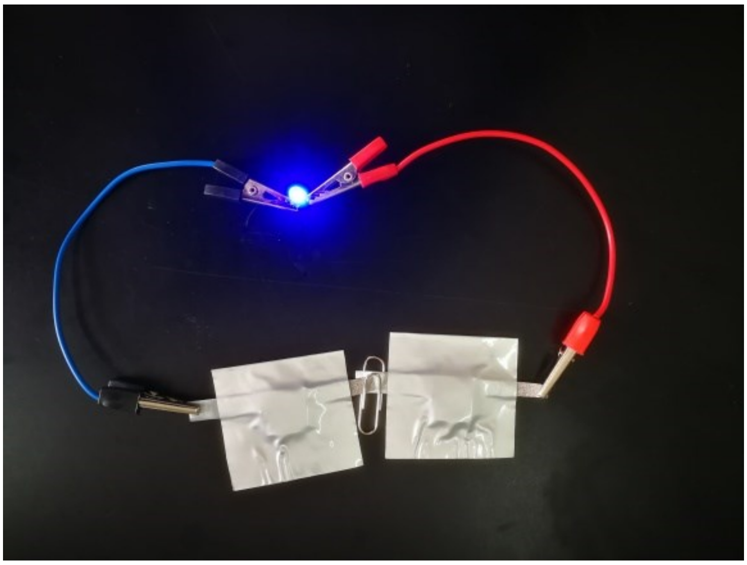

Fig. S11 Images of the Co-N-C/rGO based flexible all-solid-state ZABs in series power a light emitting diode (LED) (2.5 V)

Table S1 Comparison of ORR activities among different nonprecious catalysts in 0.1 M KOH.

Catalysts	Onset potential (V vs. RHE)	Halfwave potential (V vs. RHE)	Ref.
Co-N-C/rGO	**1.04**	**0.864**	**In this work**
S-600	0.95	0.84	Nanoscale, 2018, 10, 21076–21086
Mn–N–S–C-800	0.97	0.86	Dalton Trans., 2019, 48, 14678-14686
Co@MCM	0.95	0.86	Energy Environ. Sci., 2018, 11, 1980-1984
CoSAs/PTF-600	-	0.808	J. Mater. Chem. A, 2019, 7, 1252-1259
Co-NDC	0.89	0.81	Science Bulletin 63 (2018) 548-555
Co-POC	-	0.83	Adv. Mater. 2019, 31, 1900592
3D-Co-N-C	1.00	0.83	J. Mater. Chem. A, 2018, 6, 13050-13061
CNTs@mesoNC	0.917	0.777	J. Mater. Chem. A, 2019,7, 8975-8983
FeCNR-750	0.96	0.83	Inorg. Chem. Front., 2020, 7, 889-896
Co-NTMCs@NSC	0.945	0.833	Nanoscale, 2019, 11, 21302-21310
Co@CoS2@S/N−HCC	1.00	0.86	J. Mater. Chem. A, 2019,7, 3624-3631
NiFe@N-CFs	0.94	0.82	J. Mater. Chem. A, 2020,8,13725-13734
NGS4-900	0.984	0.859	ACS Applied Materials & Interfaces, 2018, 10, 13, 10842-10850
Co-NC-Ts	0.95	0.90	ACS Applied Energy Materials, 2020, 3, 3, 2323-2330
N-doped carbon	0.94	0.83	Adv. Mater. 2016, 28, 2337-2344.
Co3(PO4)2C-N	0.962	0.837	Energy Environ. Sci., 2016, 9, 2563-2570
Fe-N-C	0.94	0.83	ACS Nano, 2016, 10, 5922.

Table S2 Comparison of different nonprecious catalysts for HER in acidic electrolyte

Catalysts	HER Overpotential @10 mA cm^{-2}	Tafel Slope	Ref.
Co-N-C/rGO	**220**	**42**	**In this work**
B12/G800A	115	65	J. Mater. Chem. A, 2019, 7, 7179-7185
FePc-MoS2	123	32	Nanoscale, 2019, 11, 14266–14275
CoSAs/PTF-600	94	50	J. Mater. Chem. A, 2019, 7, 1252–1259
Co-NRCNTs	260	80	Angew. Chem. Int. Ed., 2014, 53, 4372-4376
FeCo@NCNTs-NH	276	74	Energy Environ. Sci., 2014, 7, 1919-1923
Co0.6Mo1.4N2	190	-	J. Am. Chem. Soc., 2013, 135, 1918 -19192
Co:WS2	240	49	Energy Environ. Sci., 2018, 11, 2270--2277
D-TiO2/Co@NCT	167	73.5	Nano Res., 2017, 10(8), 2599-2609
Multiphasic MoS2	234	46	J. Mater. Chem. A, 2017, 5, 2681-2688.
MoS2 monolayer	300	61	Adv. Mater., 2017, 29, 1701955
N/Co-doped PCP//NRGO	229	126	Adv. Funct. Mater. 2014, 201403657
Co@NC-G-700	140	-	Electrochimica Acta, 296 (2019) 830e841
FeCo@NCNTs-NH	280	74	Energy & Environmental Science, 2014, 7, 1919-1923
N,P-graphene	422	91	ACS Nano, 2014, 8, 5, 5290–5296
MoO3-MoS2	300	-	Nano Lett., 2011, 11, 10, 4168–4175
B-SuG	450	130	Catal. Sci. Technol., 2014, 4, 2023-2030